METHODOLOGIES FOR LOAD DISTRIBUTION ON A KAPLAN HYDRO TURBINE BLADE

Alexandre de Athayde Bohrer Soares
University of Brasília – Campus Universitário Darcy Ribeiro – Asa Norte
alexbohrer@hotmail.com

Dianne Magalhães Viana
University of Brasília – Campus Universitário Darcy Ribeiro – Asa Norte
diannemv@unb.br

Jorge Luiz de Almeida Ferreira
University of Brasília – Campus Universitário Darcy Ribeiro – Asa Norte
jorge@unb.br

Abstract. *The purpose of the present work is to verify the stress distribution resultant of a permanent flow, in the boundary of a Kaplan hydro turbine blade. In order to this, two distinct methodologies to obtain the pressure field over the blade were studied. The static pressure field over the blade, obtained through a simulation using the commercial software CFX 5.5.1, is compared to the static pressure field obtained by a semi-empirical method. The Computational Fluid Dynamic (CFD), simulation is based on the finite volume method. The empirical method uses an approximation of the original geometry of the blade, dividing the blade into six sections. A pressure distribution is calculated for each section, and interpolated linearly to the blade's surface, obtaining a pressure field. The static analysis was performed in the software Ansys 5.4, by the finite element method. The empiric methodology turns to be more conservative than the CFD simulation, and qualitatively similar. The empiric methodology represents a trustworthy and practical formulation to the problem of defining a static pressure field on a hydro turbine blade when other resources are not available.*

Keywords*: hydro turbine blade, pressure field, finite element method.*

1. Introduction

The recent difficulties to supply the increasing demand for electrical energy bring about the many advantages of hydro generators. This has always been one of the cheapest ways to obtain energy. Water resources are renewable and cause no atmospherical pollution. In countries like Brazil, with such abundance of water resources, the utilization of hydro-generated energy should be priority. Since the nineteenth century, hydro turbines had an incredible evolution, which associated to technological innovations permitted new applications of design and hydraulic construction. Among the technological innovations is the use of computational tools to predict and describe the fluid flow and to perform structural analysis. For economical reasons, numerical simulations are becoming more popular in the last decades, substituting tests with models of the most diversified mechanic components. Based on stress and dynamic analysis, optimized parameters can be obtained through computational tests using the finite element method and the finite volume method. In this sense, the continuous researches on fluid flow numerical simulations and its interaction with the solid structure permits improvements in the projects oh hydro turbine's components, to achieve higher efficiency and longer life (Brasil and Solomom, 2004). Numerical analyses provide good quality and precise results when you have the geometry well modeled and the correct boundary conditions imposed to the problem. The purpose of this paper is to compare the static stress distribution on a Kaplan hydro turbine blade for the pressure field obtained through a numerical simulation using the CFX software and the pressure field determined by an empirical method. For that, the computational model of the Kaplan hydro turbine's blade was built, which involved the geometry of the blade, the determination of the materials' properties, load distribution and the boundary conditions. It was used a load distribution obtained by a CFD simulation using the finite volume method in the CFX software and a load distribution obtained by the classical procedure to design axial turbines. For the second methodology, the XFoil software was used to simulate the wing sections that define the blade's geometry. The static pressure fields determined by both methodologies were compared. The static analysis using the finite element method was performed for both load conditions, to identify the stress concentration areas. This work provides important data for future analysis that intend to describe the dynamic behavior of the turbine's blade and for structural integrity analysis based on fatigue and reliability.

2. Basic theory to obtain the load on a turbine blade

The methodologies of hydraulic machine's design were developed based on the aggregation of empiric experimentally based knowledge associated to the internal theoretical hydrodynamic knowledge. These methodologies have been improved continuously together with the theoretical knowledge of fluid mechanics. In this historical process, the advanced scientific methodologies evolution's character allowed the accomplishment of complex experiments and the solution of fluid mechanics' fundamental equations. In the beginning of the twentieth century, the simplified

solution of flows, considering the hypothesis of potential flow, non viscous fluid, became part of the design of hydraulic machines (Wislicenus, 1947). The study of specific wing section for application in hydraulic machines was much diffused, and so were the techniques of definition of optimized geometry of channels and diffusers. These semi-empiric studies represent a great advance in the design methodologies. Hydraulic machines that work reasonably well, in conditions close to its ideal, have an internal hydrodynamics where the viscous effects have a much less important role than the flow topologies as defined in a first approximation by the description of potential flows. The boundary-layer theory and turbulence modeling represent an important step for the fluid dynamics evolution, and had an immediate application in the design of hydraulic machine's components. Unfortunately there are many difficulties in the practical approach of complex geometry flows, considering the non-linear effects associated to turbulence, which limited the full utilization of theoretical knowledge to the design of such machines. The fast evolution of computational methods applied to engineering changed this picture at the end of the twentieth century, permitting simulations of complex geometry and reliable results (Lakshminarayana, 1995).

2.1. Load distribution on a wing section

One of the methodologies for the design of axial turbines is the three-dimensional theory or the theory of velocity's circulation (Macintyre, 1983). It considers the assumption that the blades are far away from each other. The interaction of the elementary turbines, in which the real turbine is divided to, resembles the set of blades to a grill. The state and the trace of the blade are based on the velocity's circulation theory proposed by Kutta e Jukowsky. This theory is a generalization of the Magnus effect, applied to the domain of the wing sections. The study of an isolated blade is done in a wind tunnel, where factors are added to consider the blade confined to a reduced space. For a Kaplan hydro turbine the blade can be studied by the theory of wing sections. Suppose a wing section still and immerged in a fluid moving with linear velocity W_∞ without external interferences. The potential flow is shown in Fig. 1, where the stream lines behavior can be seen and modify their trajectory when passing by airfoil.

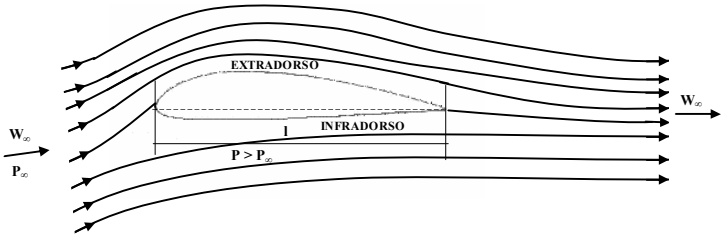

Figure 1. Actuating forces on an airfoil immerged in a potential flow.

In the upper surface the velocity of a particle is higher than the potential flow velocity, and so the pressure in the upper surface is smaller than the reference pressure P_∞. In the lower surface the velocity is smaller than W_∞ and a pressure bigger than the reference one. The following actuating forces can be identified on the airfoil: lift – force normal to the direction of the relative fluid movement; drag – force opposed to the airfoil's relative movement, following the fluid flow direction. The resultant of lift and drag forces can be decomposed in a normal force, perpendicular to the direction of the airfoil displacement and a tangential force. To calculate these force components several coefficients are used, and they vary according to the airfoil, attack angle, and are determined experimentally in wind tunnels. The Kutta-Jukowsky theory has its restrictions such as the hypothesis of potential flow, where the viscous forces are considered of small magnitude if compared to the inertial forces in high Reynolds's number flows. In a potential flow, $\boldsymbol{u}$ is an irrotational vector field; the curl of $\boldsymbol{u}$ is zero. The field $\boldsymbol{u}$ derives from a potential field Φ.

2.2. Kaplan hydro turbines

The Kaplan hydro turbines are used in small water falls and great discharge volumes. The axial turbines are appropriated for specific velocities above 350 rpm. The turbine blades can vary the operation angle, and allow a high efficiency even when working in partial discharge's regimes, with a low drop of efficiency caused by discharge variations (Macintyre, 1983). As a result of recent researches, the possibilities of application of Kaplan hydro turbines have been extended to innumerous water sources previously rejected for economical and environmental reasons (Hydraulic Turbine Catalog, Toshiba Co.). The water flow is regulated by the distributor blades and by the turbine blades inclination. The complex geometry and the transient characteristics of the flow also make more difficult to realize a simulation to capture all these singularities. These effects are extremely complex to be numerically simulated and with no analytical solution. The following methodologies provide reasonable results for the static load distribution on a Kaplan hydro turbine blade to perform the structural static analysis of the blades.

3. Methodologies to obtain the static load

Two methodologies were studied to obtain the load distribution on the Kaplan turbine blade of the hydroelectric plant of Coaracy Nunes, hydro generator 3. Table 1 shows the hydro generator's work condition studied. Data obtained from the Voith-Hydro-UHE's Manual (Voith, 1998).

Table 1. Hydro generator's work condition studied.

Working Condition		***Turbine's characteristics***	
Nominal power	29,5 MW	Stator height	2,78 m
Nominal height	21,9 m	Distributor height	1,703 m
Nominal outflow	143 m3/s	Blade's inclination angle	13°
		Distributor's opening angle	67,5°

3.1. Numerical simulation using the software CFX

The simulation was performed by LEA (Energy and Environmental Computational Laboratory, UnB), in the commercial software CFX 5.5.1. The simulation is based on the finite volume method, with a hexahedra elements mesh generated in the ICEM CFD 4.2.2 (Moura, 2003). The geometry of the rotor and blades can be visualized in Fig. 2. For the simulation was considered an inertial referential and reference pressure equals to atmospheric. The pressure field obtained can be seen in Fig. 3. The pressure in the lower surface, about 300 kPa, is larger than the pressure in the upper surface of the blade. The stagnation line can be noticed in Fig. 3 and is the region with the higher pressure values.

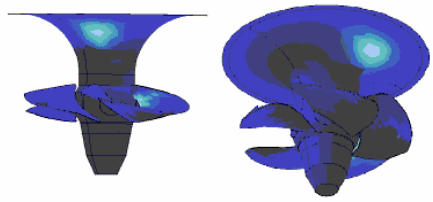

Figure 2. Rotor and blades.

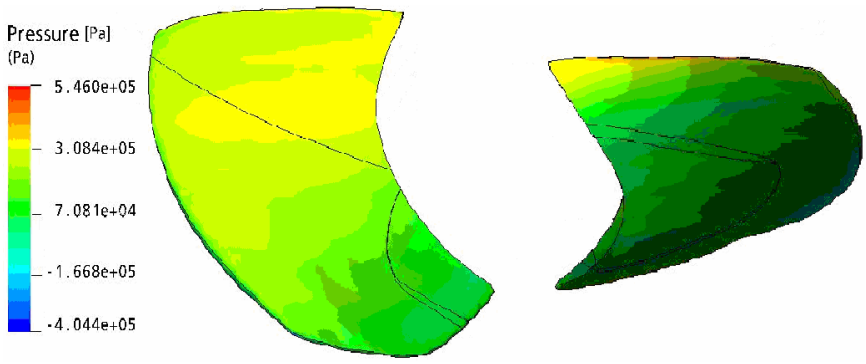

Figure 3. Pressure field obtained by the CFD simulation.

3.2. Empirical methodology

For the empirical methodology, the data was obtained by a classical procedure for axial turbine's design (Bran and Souza, 1991). These data were used in the following steps.

3.2.1. Auxiliar geometry

The blade geometry was divided into five sections by six concentric cuts. This way, five partial blades were defined. The chords (L_{CD}) for each partial blade were defined by the cut's radii, angles between the leading edge and trailing edge from the center of the cut's circumferences (θ) and the distances between the edges of the partial turbines (L). The dimensions of the partial turbine blades are calculated using the relations in Eq. 1 and are shown in Tab. 2.

$$L = 2R\sin(\theta/2) \;\; ; \; L_{CD} = R\theta \tag{1}$$

A structured triangular element's mesh was generated on the blade's surface in the pre-processor GiD. Eleven points were defined on each chord, making 132 nodes. On this nodes shall be applied the load conditions. The finite element mesh can be seen in Fig. 4.

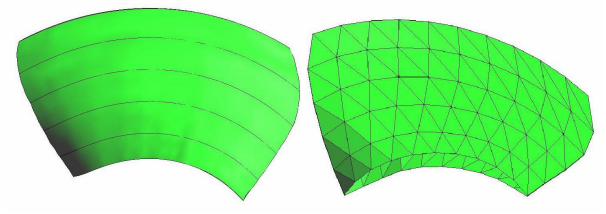

Figure 4. Concentric cuts and auxiliary triangular element's mesh.

Table 2. Dimensions of the partial turbine blades

	Radius (mm)	***L (mm)***	***θ***	***L_{CD} (mm)***
R_1	920	1557,6	2,0	1857,2
R_2	1196	1810,9	1,7	2054,3
R_3	1472	2053,5	1,5	2272,6
R_4	1748	2286,5	1,4	2492,3
R_5	2024	2420,1	1,3	2594,0
R_6	2300	2238,4	1,0	2276,5

3.2.2. Definition of the airfoils corresponding to the partial turbines

The airfoils were determined according to Mamiya and Souza (2004). The wing sections used are of Gotingen's series. From R_1 to R_3, the Go 480 airfoil is used and from R4 to R6, the Go 428 airfoil is used. To find the correspondent NACA 4 Digit airfoils you use the ratio between the maximum airfoil's thickness and its chord, and also the position where it occurs. The NACA 4 Digit Foil family was developed in 1932. For the NACA Four Digit Foil family we have: First digit - maximum camber *($y_{Cmáx}$)*; Second digit - maximum camber's location; Third e fourth digits - maximum thickness. For foils Go 428 e 480, max camber's location occurs at 30% oh the chord. The ratios of the corresponding NACA foils are presented in Tab. 3.

Table 3. NACA Foils correspondent to the Gotingen's Foils.

Gotingen Foil	$\frac{(y_S - y_I)_{máx}}{L_{CD}}$	$\left(\frac{x}{c}\right)_{Y_{Cmáx}}$ ***(%)***	***NACA 4 Digit Foil***
Go 480	0,16	30	4316
Go 428	0,05	30	4305

To simulate the partial turbines the software Xfoil will be used, and for that, the NACA Foils. The Xfoil is an airfoil's analysis code under subsonic flows, developed by Mark Drela. It is a free code, of GNU license and can be downloaded at http://raphael.mit.edu/xfoil. For the Xfoil simulation the data presented in Tab. 4 was used. This data was obtained according to Bran and Souza (1991) and Mamiya and Souza (2004).

Table 4. Data used in the Xfoil simulation.

Section	***Airfoil***	***Attack Angle (α)***	***U_∞ (m/s)***
1	NACA 4316	0,5551	12,920
6	NACA 4305	2,1108	34.987

The Xfoil furnishes C_P x *(x/c)* graphics, Fig. 5, that will be used to calculate the local pressure in the lower and upper partial turbine's surfaces.

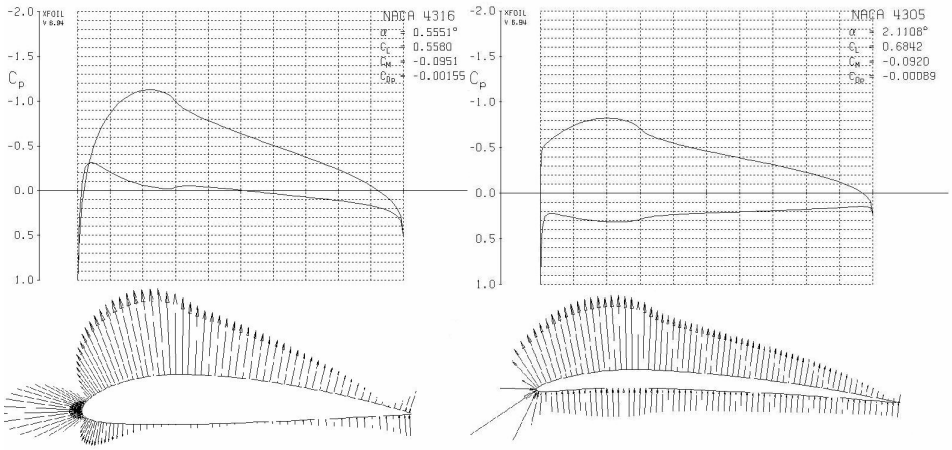

Figure 5. C_P x *(x/c)* graphics for NACA 4316 and 4305.

From the graphics shown in Fig. 5, the C_P was extracted for each 10% of the chord. The pressure was calculated for sections 1 and 6, Eq. 2. Water density was considered $\rho=1000\ kg/m^3$. With the pressure distribution for section 1 and 6, the pressure on the other sections was obtained by a linear interpolation. The empirical methodology can be used to obtain the static load on the blade for other working conditions of the turbine. The pressure field can be seen on Fig. 6.

$$P = \frac{1}{2} C_p \rho U_\infty^2 \tag{2}$$

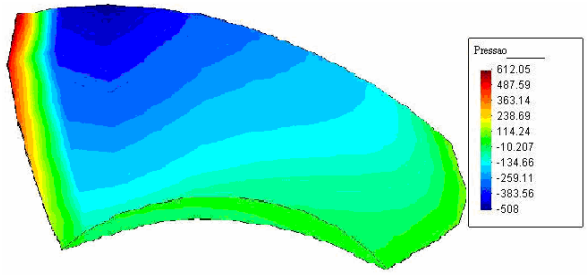

Figure 6. Pressure field (kPa) for the studied condition.

3.3. Comparison of loads distributions obtained by the two methodologies

Fifteen points were chosen on the blade's surface, as shown in Fig. 7. The pressure was compared in each point by the pressure gradient between the upper and lower surfaces. Fig. 8 shows the graphics of the pressure gradient in each of the 15 points and also the percentage difference between the gradient obtained for both methodologies according to Eq. 3.

$$dif = \frac{\Delta P_{anal} - \Delta P_{CFX}}{\Delta P_{anal}} \cdot 100 \tag{3}$$

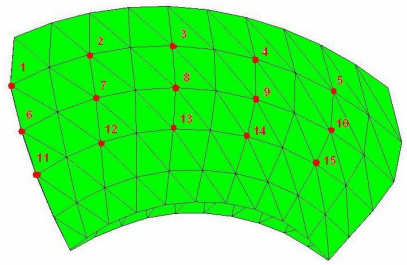

Figure 7. Points chosen for local pressure comparison between both methodologies.

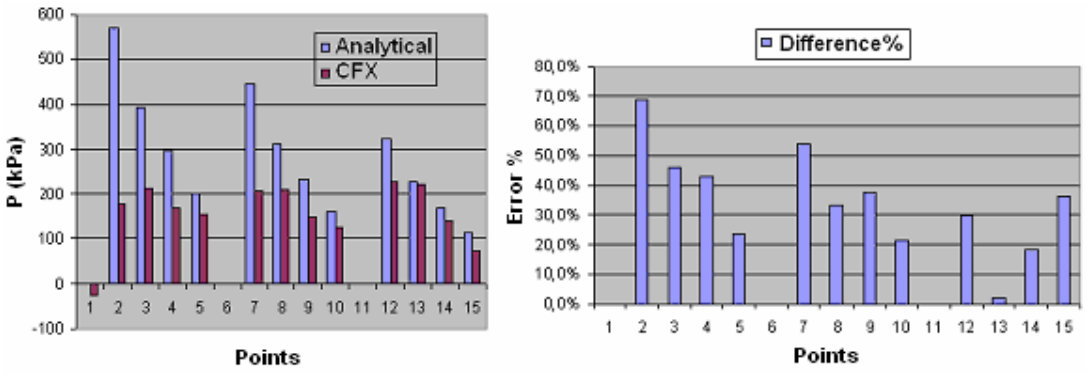

Figure 8. Pressure gradient and percentage difference between pressure gradients of both methodologies.

The larger divergence of results occurred for points 2, 7 and 12. This can be explained for the difficulty of taking accurate pressure values for the stagnation line for the CFX simulation's results. The pressure obtained corresponds to the pressure interpolated to the finite element's face closer to the selected point. The area close to the stagnation line is also the region with larger pressure gradients on the blade's surface. Observing Figs. 3 and 6, the maximum pressure is 546 kPa for the CFX simulation and 612 kPa for the empirical methodology, both in the leading edge.

4. Interpolation of the pressure fields obtained to the finite element meshes generated in GID

4.1 Finite element mesh generated in GID

The mesh was generated with tetrahedral elements, isoparametric with four nodes for element. The refinement of the meshes was emphasized in the boards and the region next to the rotor. The mesh generated and used with the load by the CFX simulation has 9649 elements and 2904 nodes. The mesh used with the load obtained by the empirical methodology has 10364 elements and 3102 nodes.

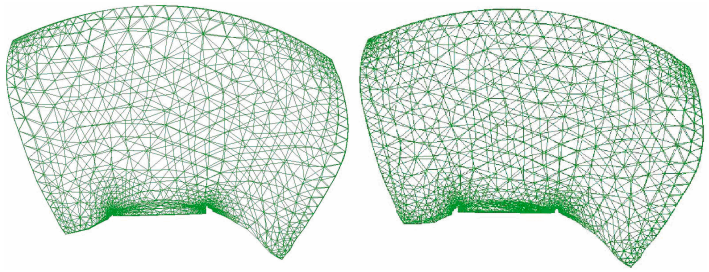

Figure 9. Mesh with 2904 nodes on the left and mesh with 3102 nodes on the right.

4.2. Interpolation of the pressure fields obtained to the meshes

For the CFX simulation the interpolation program is described in Pereira, 2003. The program interpolates the pressure furnished by the CFX's output file to the geometric center of the elements' external surfaces of the mesh generated in GID. For the program to interpolate correctly the load on the blade, both geometries, in CFX and in GID, must coincide. The mesh refinement of the fluid simulation and of the solid structure also interferes in the interpolation. The interpolation program used for the empirical methodology is similar to the used for the CFX simulation. The Tab. 7 shows the comparison of the force resultants for both methodologies. In an analogue way to the pressure, the percentage difference between the methodologies.

5. Static analysis using the finite element method

The static analysis using the finite element method was performed in the commercial software ANSYS. The mesh used in the analysis was presented in section 4 and generated in GID. The correspondent finite element in ANSYS is the Solid 72, which is an isoparametric tetrahedral element of four nodes and six degrees of freedom for each node, three rotational and three displacement d.o.f.. For the load estimative based on the CFX simulation and considering the 2904 nodes and 9649 elements' mesh, 17424 equations were generated. The Von Mises stress field and the critic region can

be seen in Fig. 11. The displacement's field can be visualized in Fig. 13. The maximum displacement is about 2,2 mm. Based on the empirical estimative of the pressure field and considering the 3102 nodes and 10364 elements' mesh, 18612 equations were generated. In Tab. 8, the results obtained with the static analysis based on these two load hypothesis can be seen. As verified, the critic region is the same for the load obtained by the CFX simulation, but with values for maximum Von Mises equivalent stress of about 200 MPa, Fig. 12. The displacement field had a similar distribution, with maximum displacement of about 3mm, Fig. 13.

Table 7. Comparison of force resultants of the pressure fields on the blade in directions x, y e z.

	F_x (N)	F_y(N)	F_z (N)
CFX	-119818	-417422	42828
Empirical Methodology	-118500	-675510	84315
Differnce= (Met. An. –CFX)/ Met. An.	-1%	38%	49%

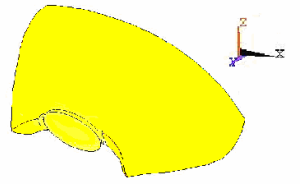

Figure 10. Coordinate reference system

Table 8. Comparison of the results obtained in the static analysis.

	$\sigma_{máx}$ Mises (MPa)	Maximum Disp.(mm)
CFX	103,517	2,195
Empirical Methodology	211,397	3,334
Diffrence= (Met. An. –CFX)/ Met. An.	51,03%	34,16%

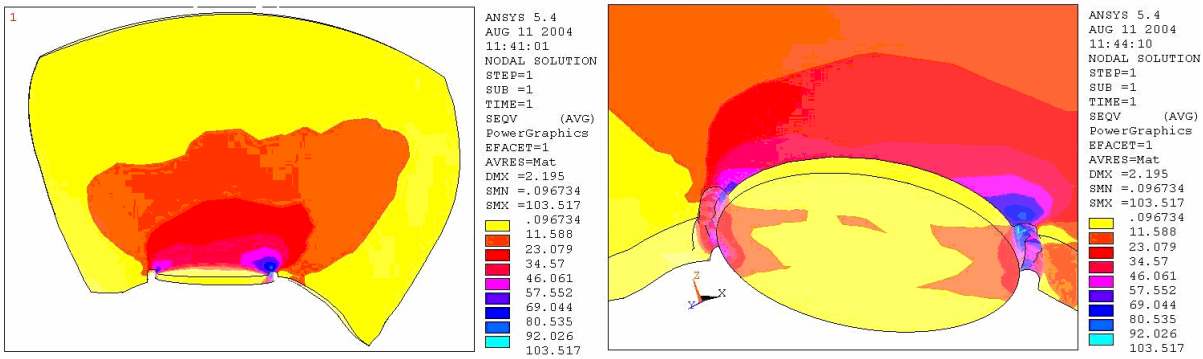

Figure 11. Von Mises stress distribution (MPa), results obtained based on the CFX simulation.

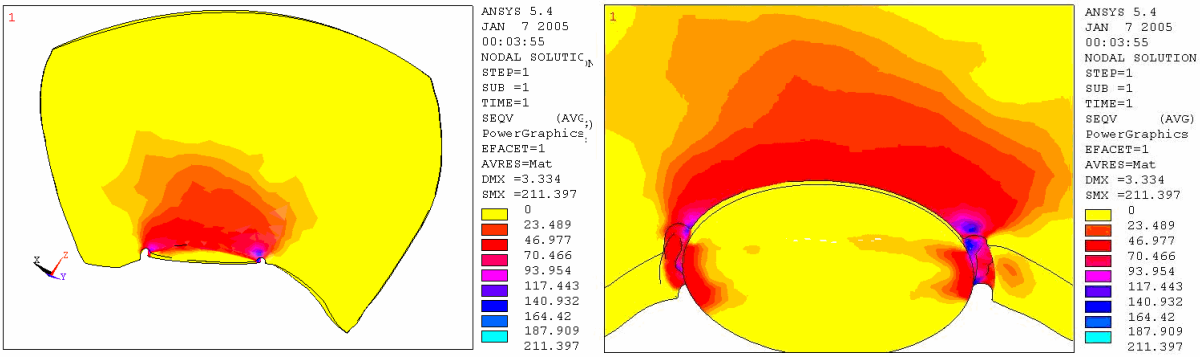

Figure 12. Von Mises stress distribution (MPa), results obtained based on empirical methodology.

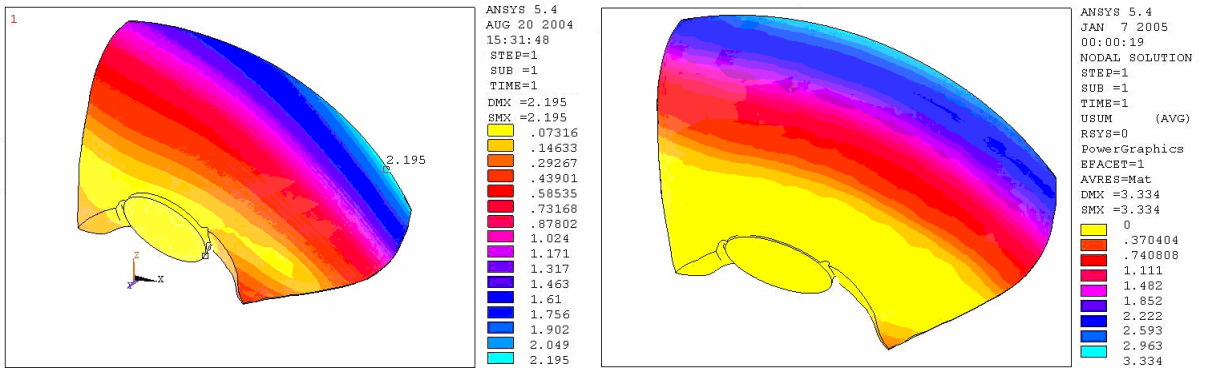

Figure 13. Displacements' field, dimensions in mm, on the left results based on the CFX simulation and on the right results based on the empirical methodology.

6. Conclusions

The results are of the same order of magnitude and it can be noticed that the regions with the biggest values of Von Mises stress and the aspect of the deformation of the blade are the same for the two cases, Figs. 11, 12 and 13. The differences in the values are attributed to the hypotheses adopted in each methodology of solution for the fluid flow. In case of impossibility of carrying through a numerical simulation for attainment of the load on the turbine blade, the empirical methodology is a practical and trustworthy alternative, because of its more conservative results. The empirical methodology also allows easily to obtain the load for others working regimes of the hydro turbine without requiring high costs or computational efforts These data could be used in future analysis to characterize the dynamic behavior of the blade and also in structural integrity analysis based on fatigue and reliability.

7. References

Arnautovic, D.; Milijanovic, R. V.,1985, "An Approach to the Analysis of Large Perturbations in Hydro-Electric Plants with Kaplan Turbines", Electric Power Systems Research, Vol. 9, pp. 115-121.

Bran, R., Souza, Z., 1991, "Máquinas de Fluxo", Ed. Ao Livro Técnico S.A., Rio de Janeiro.

Brasil, A. C. P., Solomom, L. R., 2004, "Development of Advanced Methodologies for Modernization of Hydro Turbines", Final Report, LEA - Energy and Environmental Research Group, University of Brasília, Brazil.

Lakshminarayana, B.,1995, "Fluid Dynamics and Heat Transfer in Turbomachinery", J. Wiley.

Macintyre, A. J., 1983, Máquinas Motrizes Hidráulicas, Editora Guanabara Dois, Rio de Janeiro, Brazil.

Mamiya E. N., Souza C., 2004, "Fatigue of Rotative Machines", Partial Report of UnB/Eletronorte's Project, Gamma - Mechanics of Materials Research Group, University of Brasília, Brasília, Brazil.

Moura, M. D., 2003, "Assessment of Turbulence Modeling for CFD Simulation in Hydroturbines: Draft Tube", In: International Congress of Mechanical Engineering, Proceedings of 17th. COBEM, São Paulo, Brazil.

Pereira, R. M., 2003, "Meshless Interpolation Applied to Fluid Structure Interaction", In: International Congress of Mechanical Engineering, Proceedings of 17th. COBEM, São Paulo, Brazil.

Wislicenus, G. F., 1947,"Fluid Mechanics of Turbomachinery", McGraw-Hill.

Toshiba Corporation , 20??, "Hydraulic Turbines Catalog", Vol. 6316-5.

Voith-Hydro-UHE, 1998, "UHE Coaracy Nunes Manual", Machine Number 3.

8. Responsibility notice

The authors are the only responsible for the printed material included in this paper.